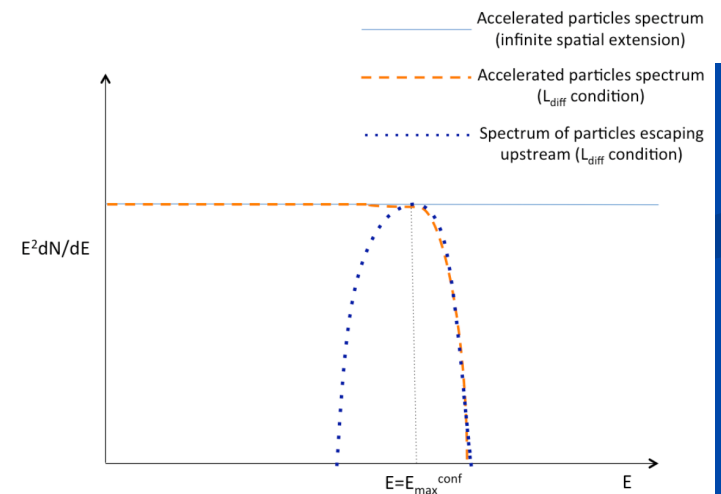


Lecture 18 051219

Il pdf delle lezioni puo' essere scaricato da
[http://www.fisgeo.unipg.it/~fiandrin/didattica_fisica/
cosmic_rays1920/](http://www.fisgeo.unipg.it/~fiandrin/didattica_fisica/cosmic_rays1920/)

At different times of the shock propagation, the spectrum of escaping cosmic-rays looks like the one displayed in Fig. 3.11, relatively hard and narrow. The instantaneous spectrum of escaping cosmic-rays is then very different (much harder) from the spectrum of the accelerated cosmic-rays ($\propto E^{-2}$ we obtained with the DSA mechanism in the previous chapter. More importantly, it is also very different from the source spectrum which is deduced from the energy evolution of the abundance of LiBeB elements (see Chapt. 2 and Eqs. 2.17 and 2.22, $n(R) = q(R)\tau_{esc}(R) \propto R^{-(\alpha+\beta)}$ with $\alpha = 0.3 - 0.6$ index of the rigidity evolution of the cosmic-ray confinement time in the Galaxy and $\beta = 2.1 - 2.4$ spectral index at the sources). It makes however more sense to compare the source spectral index ($\beta = 2.1 - 2.4$, obtained from cosmic-ray composition measurements) with the spectrum of escaping cosmic-rays integrated over the whole time evolution of the SNR. Indeed, in the hypothesis that SNRs are the main sources of Galactic cosmic-rays then the cosmic-ray spectrum we observe today on Earth would be the sum of the contribution of many different SNR of different age and since the cosmic-ray propagation is diffusive, it is also possible that at a given observation time we could receive cosmic-rays coming from a same SNR but which have escaped at very different epochs of the SNR evolution.



Different studies either numerical or analytic have been performed in order to estimate the time integrated spectrum of cosmic-rays escaping from a SNR. Although these calculations unavoidably rely on assumptions and simplifications it seems that it is possible for the time integrated spectra of escaping cosmic-rays to be compatible with what is required (*i.e* a spectral index $\beta = 2.1$) to make the SNR hypothesis compatible with observations. In any case, we see that, the discussion of the spectrum of cosmic-ray emitted by their possible source goes way beyond the apparent simplicity and universality of the spectrum of accelerated cosmic-ray obtained deriving the DSA mechanism.

Non trivial issues

In this paragraph we will discuss/mention some considerations which go beyond the simple model of the diffusive shock acceleration we derived in the previous chapter but are relevant for the discussion of the origin of Galactic cosmic-ray. Since these discussions make use of relatively advanced notions we will limit ourselves to a very brief discussion.

(i) In the previous chapter, in the version of the DSA mechanism we derived, we neglected the back reaction of the accelerated cosmic-rays on the shock. Such a back reaction is expected to take place when the fraction of the total energy available which is communicated to cosmic-rays is significant (which is supposedly the case in SNRs). In this case, the pressure due to cosmic-rays is expected to modify the physical conditions at play in the vicinity of the shock. Deviations with respect to the universal spectral index $x = 2$ are expected. This issue is currently matter of intense activity in the community. As non linear theories of CR acceleration

Non trivial issues

(ii) Particles injection : As briefly mentioned in the previous chapter, astrophysical shocks are "collisionless" (or non-collisional) and all the energy dissipation at the shock occurs by interactions between the magnetic turbulence carried by the shock and the ambient charged particles. The associated microphysics is beyond the scope of this course, let us note however, that the shock thickness is expected to be of the order of a few Larmor radii of the ambient thermal ions (which carry a lot more momentum than the ambient thermal electrons). To be accelerated, particles must see the shock as a discontinuity which implies that particles must have a Larmor radius initially significantly larger than the shock radius. This condition is in principle fulfilled by ions which are in the high energy tail of the thermal (Maxwellian) distribution. In the case of electrons, the situation is more complicated since thermal electrons have smaller momentum/rigidity/Larmor radii than thermal ions, the question of the injection of electrons at the shock is then highly non trivial... For that reason, it is usually thought that accelerated electrons receive much less energy from the shock than the accelerated ions.

Moreover, let us note that the non-trivial question of particle injection at a shock has also some interesting consequences regarding the relative abundances of the different ionic species as we will discuss later.

Energy losses

So far the acceleration mechanisms we presented, as well as the escape of particles, depended only on the rigidity of the particles and the behavior of protons, nuclei and electrons at a given rigidity was expected to be the same. We expect for instance, the maximum energy of accelerated and escaping protons and electrons to be the same and to be proportional to the atomic number Z for nuclei. This "symmetry" between electrons, protons and other ions is expected to be broken by energy losses that the different species experience during their acceleration and escape, be it in a SNR or in any other type of astrophysical source.

An additional limitation to maximum energy reachable is met when $t_{acc}(E) = t_{loss}(E)$, ($t_{loss}(E)$ being the energy loss time due to a given energy loss process or the sum of different loss processes, see below). We use here for the first time the energy rather than the rigidity since we do not expected electrons, protons and nuclei to behave the same way with respect to energy losses. For a given

Energy losses

For a given

species, energy losses become a limiting factor whenever E_{max}^{loss} , the energy such that $t_{acc}(E_{max}^{loss}) = t_{loss}(E_{max}^{loss})$, is lower than $E_{max}^{age} = Z \times R_{max}^{age}$ or $E_{max} = Z \times R_{max}^{conf}$. We will see that we expect this to be the case for electrons in SNRs, but not for protons or nuclei. Obviously for different type of astrophysical sources, the competition between the different causes of limitation of the maximum achievable energy has to be studied case by case for electrons, protons and nuclei⁶.

The formal definition for a given energy loss process i is :

$$t_{loss}^i(E) = \left(-\frac{1}{E} \left(\frac{dE}{dt}(E) \right)_i \right)^{-1} \quad (4.7)$$

when several energy loss processes have to be considered, we have :

$$t_{loss}^{total}(E) = \left(\sum_i \frac{1}{t_{loss}^i(E)} \right)^{-1} \quad (4.8)$$

Adiabatic losses

All charged particles in a supernova remnant (and in all expanding medium in general) are expected to experience adiabatic losses due to the expansion of the remnant. The gas does work during the expansion and its internal energy decreases : $dU = -PdV$ where U is the internal energy, P the gas pressure and V the volume. For a monoatomic gas $U = \frac{3}{2}nkJTV$ and $p = nkT$, with n being the particle density, T their temperature and k the Boltzmann constant, (the average energy per particle then being $\frac{3}{2}kT$). We then have, $dU = nVdE = -\frac{2}{3}nEdV$ and hence, $\frac{dE}{dt} = -\frac{2nE}{3N} \frac{dV}{dt}$, with $N = nV$.

$\frac{dV}{dt}$ is the expansion rate of the volume, which is related to the velocity field $\vec{v}(\vec{r})$. Let us now assume the volume is a cube, we can describe the change of the volume by the differential expansion of the three pairs of faces :

$$\frac{dV}{dt} = (v_{x+dx} - v_x)dydz + (v_{y+dy} - v_y)dx dz + (v_{z+dz} - v_z)dxdy \simeq \left(\frac{\partial v_x}{\partial x} + \frac{\partial v_y}{\partial y} + \frac{\partial v_z}{\partial z} \right) dxdydz = (\vec{\nabla} \cdot \vec{v})V \quad (4.9)$$

in the limit of small dx, dy, dz . We thus get, $\frac{dE}{dt} = -\frac{2}{3}(\vec{\nabla} \cdot \vec{v})E$.

For relativistic particles the energy per particle is $E = 3kT$, we thus get $\frac{dE}{dt} = -\frac{1}{3}(\vec{\nabla} \cdot \vec{v})E$.

Adiabatic losses

In the case of SNRs and more generally for astrophysical shock waves, we are dealing in good approximation, with uniformly expanding sphere, the velocity field is then $v(r) = v_0(r/R_{sphere})$, where R_{sphere} is the radius of the sphere and v_0 is the velocity at the outer radius R_{sphere} . In that case, we have $\vec{\nabla} \cdot \vec{v} = 3(v_0/R_{sphere})$ then for relativistic particles confined within the sphere we have :

$$-\left(\frac{dE}{dt}\right)_{exp} = \left(\frac{v_0}{R_{sphere}}\right) E = \left(\frac{1}{R_{sphere}} \frac{dR_{sphere}}{dt}\right) E \Leftrightarrow -\frac{1}{E} \left(\frac{dE}{dt}\right)_{exp} = \left(\frac{1}{R_{sphere}} \frac{dR_{sphere}}{dt}\right) \quad (4.10)$$

Adiabatic losses

The energy loss time is then $t_{loss}^{exp}(E) = \frac{\dot{R}_{sphere}}{R_{sphere}}$, which for a SNR within our notations corresponds to $t_{loss}^{exp}(E) = \frac{v_{sh}}{R_{sh}}$ which is equivalent to the age of the SNR in the free expansion phase. Adiabatic losses are then not a more limiting factor than the age of the SNR for the accelerated particles. Particles which are accelerated and manage to escape from the source will then not be very significantly affected by adiabatic losses. On the other hand, those which are accelerated but remain trapped within the SNR (because the rigidity they reached before being advected downstream of the shock is much lower than the R_{max}^{conf}) are likely to lose most of their energy while they are confined. Note that this energy is however not totally lost as far as cosmic-ray acceleration is concerned. It participates to the expansion of the SNR and might serve at later times to accelerate new cosmic-rays.

To conclude on adiabatic losses, let us note that the energy energy loss time is independent of the energy and that this process affects all types of relativistic charged particles the same way (protons, nuclei and electrons) and thus does not by itself break the symmetry in the behaviour of the different type of particles at a given rigidity.

Energy losses of electrons

Besides adiabatic losses, electrons are going to be affected by many different energy loss processes during their acceleration. To be more precise, these energy loss processes are not specific to electrons, they also affect protons and nuclei but in the case of SNR they are only significant for the case of electrons⁷. Among the most significant energy loss processes for electrons, one can cite :

- (i) Ionisation losses
- (ii) Bremsstrahlung losses
- (iii) Synchrotron losses
- (iv) Inverse compton losses

The first two processes are not too important in general in the case of SNR and we overlook them in the following. Note that all these processes are described in much more details in two very pedagogical books (in particular all the formulas we will give below are derived in all details), M. Longair's *"High Energy Astrophysics"* and Rybicki and Lightman's *"Radiative Processes in Astrophysics"*.

Synchrotron losses

In most cases, the most important energy loss process for electrons is the synchrotron emission which corresponds to the emission of an accelerated charged particle in the presence of an ambient magnetic field. It can be shown that :

$$-\left(\frac{dE}{dt}\right)_{syn} = \frac{4}{3}\sigma_T c \gamma^2 U_{mag} \quad (4.11)$$

where σ_T is the Thomson cross section, γ is the electron Lorentz factor and $U_{mag} = \frac{B^2}{2\mu_0}$ (S.I) = $\frac{B^2}{8\pi}$ (C.G.S) is the magnetic field energy density.

⁷In astrophysical sources where magnetic fields might be very strong, for instance in the nuclei of an AGN or a gamma-ray bursts, synchrotron losses become important for protons and nuclei (see below).

Synchrotron losses

For the energy loss time of the electrons by synchrotron losses, we get the following scaling law

$$t_{loss}^{syn}(E_e) = \left(-\frac{1}{E_e} \left(\frac{dE_e}{dt}(E_e) \right)_{syn} \right)^{-1} \simeq 1.2 \times 10^4 \left(\frac{B}{\mu\text{G}} \right)^{-2} \left(\frac{E_e}{10^{15} \text{ eV}} \right)^{-1} \text{ yr} \quad (4.12)$$

It can also be demonstrated that the typical energy of the synchrotron photons produced by an electron of energy E_e in a magnetic field B is given by :

$$E_{\gamma}^{syn}(E_e) \simeq 6.7 \times 10^4 \left(\frac{E_e}{10^{15} \text{ eV}} \right)^2 \left(\frac{B}{\mu\text{G}} \right) \text{ eV} \quad (4.13)$$

Let us add that the spectrum of photons produced by a population of electron is related to the spectrum of the parent population of electrons. Assuming the electrons are following a power law spectrum of index p : $n(E_e) \propto E_e^{-p}$, then the produced photon spectrum will also follow a power law : $n_{\gamma}(E_{\gamma}) \propto E_{\gamma}^{-\frac{p+1}{2}}$, *i.e* with a spectral index $\frac{p+1}{2}$.

Synchrotron losses

Let us come back to the case of a SNR with $B = 100 \mu\text{G}$ and $v_{sh} = 3000 \text{ km.s}^{-1}$ we see that $t_{loss}^{syn}(E_e = 10^{15} \text{ eV}) \simeq 1.2 \text{ yr} \ll t_{acc}(E_e = 10^{15} \text{ eV}) \simeq 480 \text{ yr}$. The energy for which $t_{loss}^{syn}(E_e) = t_{acc}(E_e)$ can be calculated, we see immediately that $E_{max}^{loss, syn} < 10^{14} \text{ eV}$ which means that the acceleration of electrons in a SNR will indeed be limited by synchrotron losses. If one assumes a stronger magnetic field, the situation only gets worse since $t_{loss}^{syn}(E_e) \propto B^{-2}$ while $t_{acc}(E_e) \propto B^{-1}$.

Let us now come back to the case of the SNR we considered earlier keeping the same physical parameters $B = 100 \mu\text{G}$, $v_{sh} = 3000 \text{ km s}^{-1}$, and the same time evolution using a free expansion phase duration of 480 years. Let us first calculate the value $E_{e max}^{loss, syn}$, the maximum energy of the electrons due to synchrotron losses, during the free expansion phase. Let us note that since the magnetic field is assumed to be constant during this phase then $E_{e max}^{loss, syn}$ should also be constant during the free expansion phase. Fixing $B = 100 \mu\text{G}$, we then have $t_{loss}^{syn} \simeq 1.2 \left(\frac{E}{10^{15} \text{ eV}} \right)^{-1}$ and $t_{acc} \sim 480 \text{ yr} \left(\frac{E}{10^{15} \text{ eV}} \right)$. Equating the two times gives us $E_{e max}^{loss, syn} \simeq 5 \cdot 10^{13} \text{ eV}$. This value of the maximum energy will hold till the end of the free expansion phase. To know the evolution of $E_{e max}^{loss, syn}$ during the Sedov-Taylor phase, we just have to calculate the scaling with time since we already know the value at the beginning of this phase :

Synchrotron losses

We have during the Sedov-Taylor phase, $t_{acc}(E_e) \propto E_e B^{-1} v_{sh}^{-2}$ and $t_{syn}(E_e) \propto E_e^{-1} B^{-2}$ which means, using the time evolution of B and v_{sh} , that $(E_{e\ max}^{loss, syn})^2 \propto B^{-1} v_{sh}^2 \Leftrightarrow E_{e\ max}^{loss, syn} \propto t^{-3/10}$. Summarising our results we have⁸ :

$$E_{e\ max}^{loss, syn}(t) \simeq 5\ 10^{13}\ \text{V for } t \leq 480\ \text{yr} \quad (4.14)$$

and

$$E_{e\ max}^{loss, syn}(t) \simeq 5\ 10^{13} \times \left(\frac{t}{480\ \text{yr}} \right)^{-3/10} \text{V for } t > 480\ \text{yr} \quad (4.15)$$

The evolution of $E_{e\ max}^{loss, syn}$ is shown in Fig. 4.3 and is compared to the evolution of E_{max}^{conf} and E_{max}^{age} allowing us to understand qualitatively the fate of the accelerated electrons during the whole SNR evolution.

Maximum energy : radiative limit

- For an electron radiative losses oppose acceleration

$$\frac{dE}{dt} = -bU^2 E^2 \quad \text{with } U = B^2/2\mu_0$$

- **Radiative limit**

- E_{max} is reached when $\dot{E}_{acc} + \dot{E}_{rad} = 0$
- Using t_{acc} :

$$\dot{E}_{acc} = bU_B E_{max}^2 \Rightarrow E_{max} = \left(\frac{\dot{E}_{acc}}{bU} \right)^{1/2}$$

$$E_{max,rad} = \left(\frac{3}{2} \frac{r-1}{r(r+1)} \frac{e\mu_0}{\sigma_T c B} \right)^{1/2} V_s m_e c^2$$

- For a typical SNR :

$$E_{max,rad} = 240 \text{ TeV} \left(\frac{V_s}{10^4 \text{ km/s}} \right) \left(\frac{B}{1 \text{ nT}} \right)^{-1/2}$$

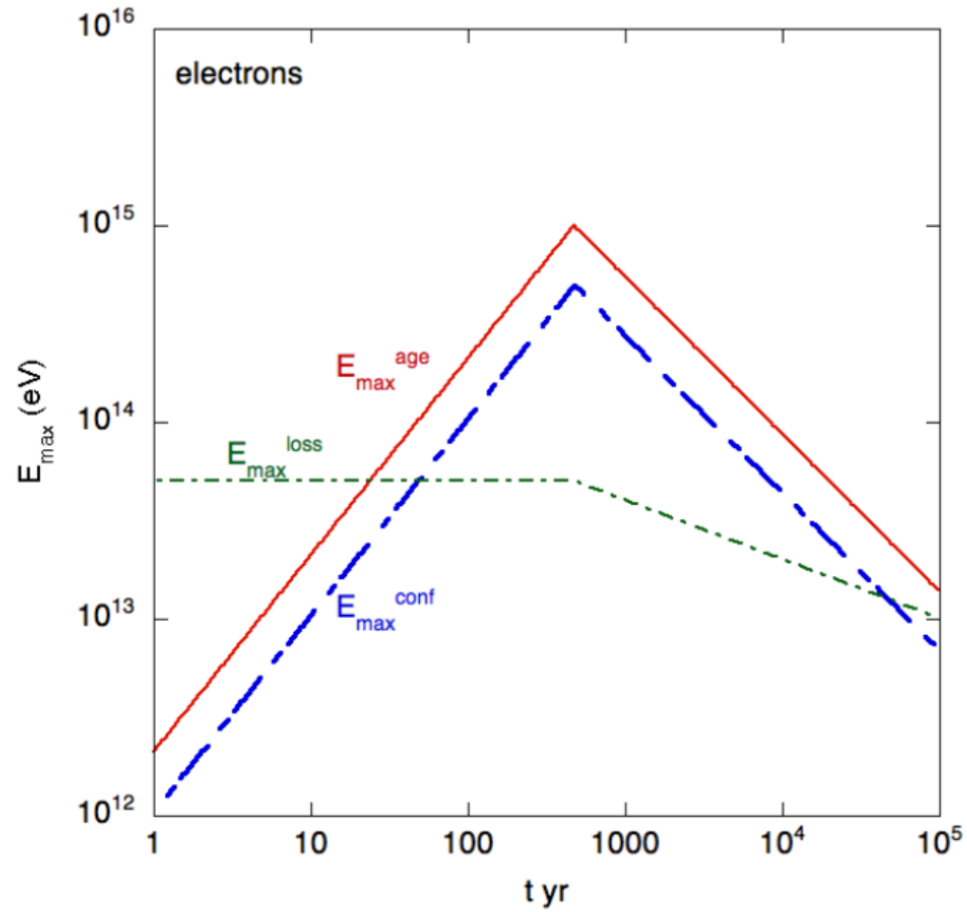


FIG. 4.3: Comparison of the time evolution of $E_{e \max}^{\text{loss, syn}}$, E_{\max}^{conf} and E_{\max}^{age} of the accelerated electrons for our toy model parameters (see text).

Synchrotron losses

During the beginning of the free expansion phase, $E_{e\ max}^{loss, syn}$ is larger than E_{max}^{conf} and E_{max}^{age} , as a result synchrotron losses are not a limiting factor for the acceleration of electrons and those with $E_e \simeq E_{max}^{conf}$ manage to escape to the ISM. This situation lasts roughly 50 years and then $E_{e\ max}^{loss, syn}$ becomes smaller than E_{max}^{conf} and E_{max}^{age} . In this case the acceleration of electrons is limited by synchrotron losses and moreover the electrons remain trapped in the SNR since $E_{e\ max}^{loss, syn}$ becomes rapidly significantly smaller than E_{max}^{conf} . This situation holds for the rest of the SNR evolution although with our hypothesis E_{max}^{conf} and E_{max}^{age} decrease more rapidly than $E_{e\ max}^{loss, syn}$ during the Sedov phase⁹.

This illustration demonstrate that synchrotron losses of electrons are a limiting factor for their acceleration during most of the evolution and incidentally these energy losses result in the production of ample fluxes of photons which as discussed earlier can be used to constrain the shape of the spectrum of the accelerated electrons (as well as some of the source parameters as we will see in the next few paragraphs).

Synchrotron losses

Finally it is worth mentioning that for a nuclear species of mass M and atomic number Z , the synchrotron loss time can be deduced from that of an electron of the same energy :

$$t_{syn}(E, M, Z) = \left(\frac{M}{m_e}\right)^4 \frac{1}{Z^4} t_{syn}(e^-, E_e = E) \quad (4.16)$$

Since $m_p/m_e \simeq 1836$ we immediately see that synchrotron losses will be negligible for protons and nuclei in SNRs.

Inverse Compton Losses

The energy lost per unit time by the inverse Compton process is given by :

$$-\frac{dE}{dt}(\gamma_e) = \frac{3}{4}\sigma_T c \gamma_e^2 U_{rad} \quad (4.18)$$

Where U_{rad} is the radiation energy density (for instance $U_{CMB} \simeq 0.25 \text{ eV cm}^{-3}$)

It yield for the energy loss time :

$$t_{loss}^{ICS}(\gamma_e) \simeq \frac{2.3 \times 10^{12}}{\gamma_e} \left(\frac{U_{rad}}{U_{CMB}} \right)^{-1} \text{ yr} \quad (4.19)$$

Let us note that in the ISM, synchrotron and inverse Compton losses are comparable while in a typical SNR synchrotron losses are far more important due to the amplified magnetic fields at play.

Inverse Compton Losses

There are basically two regimes for inverse Compton losses and photon emission depending on the above mentioned center of mass energy s .

(i) The Thomson regime is relevant when $s \simeq m_e^2 c^4$, we have in this case $\sigma_{ICS} \simeq \sigma_T$. In this case a photon with initial energy E_γ^{ini} is expected to be boosted to an energy $E_\gamma^{final} \simeq \gamma_e^2 E_\gamma^{ini}$ where γ_e is the Lorentz factor of the electron.

(ii) The Klein-Nishina regime is relevant when $s \gg m_e^2 c^4$. In this regime the cross section falls rapidly with s as $\sigma_{ICS} \propto s^{-1}$ and one gets $E_\gamma^{final} \simeq E_e$ meaning that the energy loss becomes catastrophic for the electron. Let us note that since we saw that the maximum energy of electrons in a SNR was quite unlikely to reach values larger than 10^{14} eV due to synchrotron losses then photons from ICS interactions in the Klein-Nishina regime are also very unlikely to reach these energies. This observation will actually be extremely relevant when we will discuss the possibility of distinguishing between high energy photons produced by high-energy electrons from those produced by high-energy cosmic-rays (see below).

Inverse Compton Losses

Like in the case of photons produced by synchrotron losses, the expected photon spectrum is related to the spectrum of the accelerated electron population which boosted them. Assuming again the accelerated electrons are following a power law spectrum of index p : $n(E_e) \propto E_e^{-p}$, then the produced photon spectrum will also follow a power law spectrum : in the Thomson regime, $n_\gamma(E_\gamma) \propto E_\gamma^{-\frac{p+1}{2}}$, and in the Klein-Nishina regime, $n_\gamma(E_\gamma) \propto E_\gamma^{-(p+1)}$.

Let us note that in some cases, the photons which are being boosted by the accelerated electrons might be the very same photons which have been produced by the same population of electrons due to synchrotron losses. In this case, the ICS process is rather called synchrotron self-Compton or SSC¹⁰.

¹⁰Let us note that the ICS and synchrotron processes are always competing in astrophysical sources. If for instance the magnetic field is too strong and the high energy electrons lose their energy too rapidly by synchrotron losses then these "cooled" electrons are not available anymore to produce ICS photons in the Klein-Nishina regime and the latter process is then highly suppressed.

In the case of protons and nuclei the ICS process is totally negligible.

Energy losses of protons and nuclei

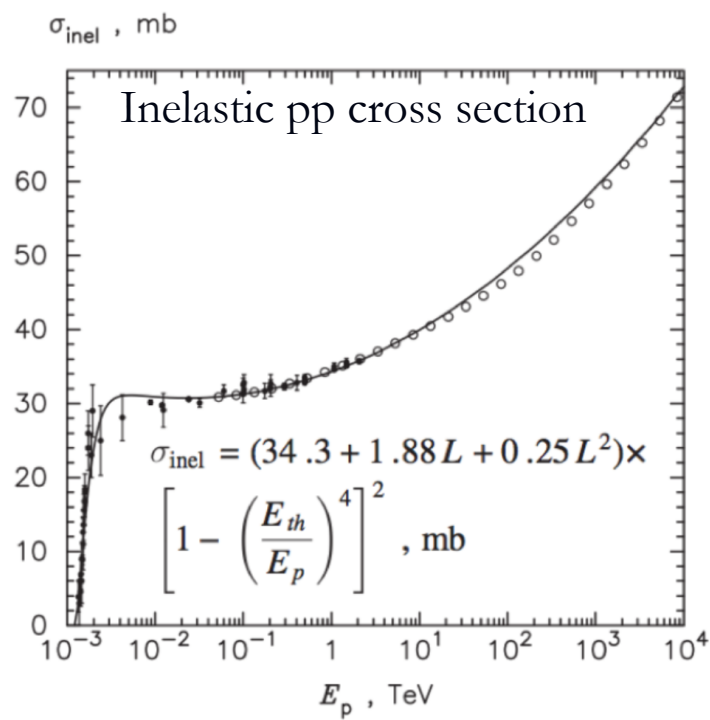
As discussed above, protons and nuclei suffer from adiabatic losses but remain quite insensitive to synchrotron (at least in SNRs) and ICS losses. The main interaction channel for protons and nuclei takes place through hadronic interactions¹¹ with the ambient matter (mainly H and He atomic nuclei) which is in good approximation at rest. In the case of protons, above a certain energy threshold pions can be produced (see below) while nuclei suffer from spallation reactions (see Chapt. 2) and may also emit pions.

Let us concentrate on the proton case (so-called pp interactions). A collision between an accelerated proton and an ambient proton or He at rest gives in most cases a pion (either charged or neutral) :

$$p + p \rightarrow p + p + \pi^0 \Rightarrow \pi^0 \rightarrow 2\gamma \quad (4.20)$$

$$p + p \rightarrow p + p + \pi^+ \Rightarrow \pi^+ \rightarrow \mu^+ + \nu_\mu \Rightarrow \mu^+ \rightarrow e^+ + \bar{\nu}_\mu + \nu_e \quad (4.21)$$

$$p + p \rightarrow p + p + \pi^- \Rightarrow \pi^- \rightarrow \mu^- + \bar{\nu}_\mu \Rightarrow \mu^- \rightarrow e^- + \nu_\mu + \bar{\nu}_e \quad (4.22)$$



Energy losses of protons and nuclei

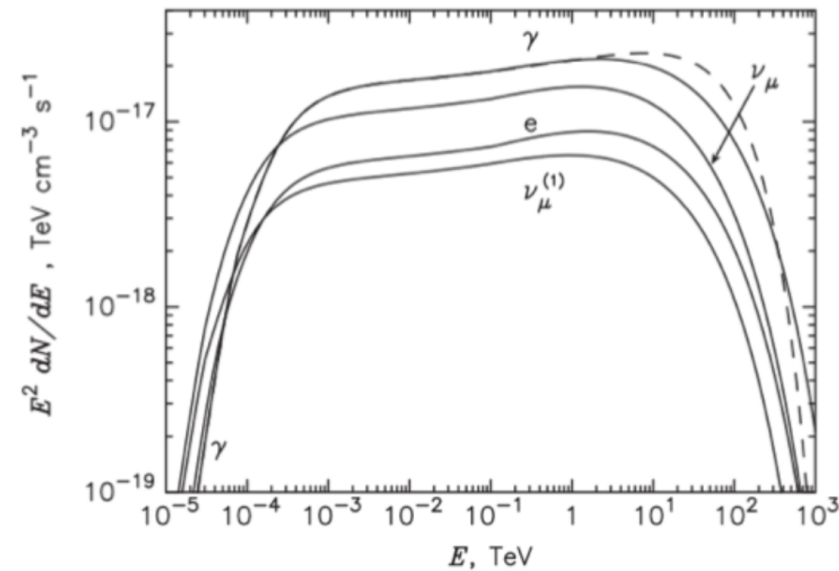
The energy threshold to produce a π^0 in pp interactions is :

$$E_p^{th} = m_p + \frac{m_{\pi^0}}{m_p} \left(2m_p + \frac{m_{\pi^0}}{2} \right) \simeq 1.22 \text{ GeV} \quad (4.23)$$

which correspond to a kinetic energy of the proton $T_p^{th} \simeq 280 \text{ MeV} \simeq 2m_{\pi^0}$.

In good approximation, the produced π^0 carries in average $\sim 17\%$ of the accelerated proton initial energy which redistributed to the 2 photons immediately produced in the π^0 decay. The pp cross section shown in Fig. 4.4a is quasi constant with the energy (hardly rising by a factor of two over 7 orders of magnitude of the proton energy), for the following orders of magnitude calculations we will assume the cross section to be constant at 50 mbarn.

Energy losses of protons and nuclei



Spectrum of photons, electrons, neutrinos (electronic and muonic) produced by the interaction of protons distributed as a power law spectrum $n(E) \sim E^{-2}$ with an exponential cut-off above 10^{14} eV (100 TeV).

The spectrum of outgoing photons, neutrinos and electrons after pp interactions are shown in Fig. 4.4b, assuming an initial spectrum of accelerated protons $n(E_p) \propto E^{-2}$ and an exponential cut-off above 10^{14} eV (100 TeV). The resulting photon spectrum has practically a shape in $n(E_\gamma) \propto E_\gamma^{-2}$, although slightly harder (*i.e.* $p \leq 2$) due to slight increase of the pp cross section with E_p . We also see that the photon spectrum shows an exponential cut-off around ~ 10 TeV (10^{13} eV) which is expected since photons carry roughly a bit less than 10% of the initial accelerated proton energy (and the proton spectrum was assumed to present an exponential cut-off above 100 TeV). Note that the situation of the produced neutrinos is qualitatively the same except that these neutrinos are expected to carry 3-5% of the energy of the primary proton.

Energy losses of protons and nuclei

With the cross section being known, one can calculate the mean interaction time $t_{int}^{pp} = (n\sigma_{pp}c)^{-1}$. Using $\sigma_{pp} \simeq 50$ mbarn (and constant), we get

$$t_{int}^{pp} \simeq 2.1 \times 10^6 \left(\frac{n}{10 \text{ cm}^{-3}} \right)^{-1} \text{ yr} \quad (4.24)$$

since in average 17% of the proton energy is lost during a single interaction we get for the loss time t_{loss}^{pp} ,

$$t_{loss}^{pp} \simeq 10^7 \left(\frac{n}{10 \text{ cm}^{-3}} \right)^{-1} \text{ yr} \quad (4.25)$$

The loss time is much larger than the time a SNR remain active. It means that hadronic interactions are never a limiting factor for the acceleration of protons (it remains true for nuclei, the cross section being roughly proportional to $A^{2/3}$). However, the photons which are emitted during the interactions (which are unlikely during the acceleration of a single proton or nuclei but must occur within a large population of accelerated protons and nuclei) can be used as a signature of the presence of accelerated cosmic-ray protons and nuclei.

Leptonic/hadronic γ emission

The produced photons will however have to compete with those emitted by electrons in the same energy range. Even though electrons are in principle discriminated at the injection at the shock (see the paragraph on "non-trivial issues") with respect to protons and nuclei, they radiate so much more efficiently that it is always quite challenging to find protons and nuclei acceleration signatures in the photon spectra emitted by SNRs. We will see a few examples in the next paragraphs.

Leptonic/hadronic γ emission: RX J0852.0-4622 (Vela-Jr) SNR

The complexity of the interpretation of photon spectra observed from SNRs can be illustrated by the case of the SNR RX J0852.0-4622 also called Vela-Jr shown in Fig. 4.5. This SNR has been observed in radio, X-rays and very high energy γ -rays (by the HESS observatory)¹². The SNR distance and the physical environment (matter density, magnetic fields) are not very well constrained by observations. In the case, there is a large room to model the γ -ray emission and Fig. 4.5 shows two different models which can be considered as acceptable fits of the data. The left panel assumes a predominantly "leptonic" origin (*i.e* a majority of photons emitted by accelerated electrons) of the γ -ray assuming a relative small value of the field $B = 6 \mu\text{G}$ (so more or less comparable with that of the ISM) in the acceleration region, together with a low matter density $8 \cdot 10^{-3} \text{ cm}^{-3}$ to favor inverse Compton emission over π^0 decay. On the other hand, the right panel with much larger magnetic field $B = 85 \mu\text{G}$ and density $d = 2 \text{ cm}^{-3}$ (closer to the standard value expected especially in the context of amplified magnetic fields at the shock) implies a dominant contribution of "hadronic" γ -rays (*i.e* produced by hadronic interactions) from the decay of π^0 .

Leptonic/hadronic γ emission: RX J0852.0-4622 (Vela-Jr) SNR

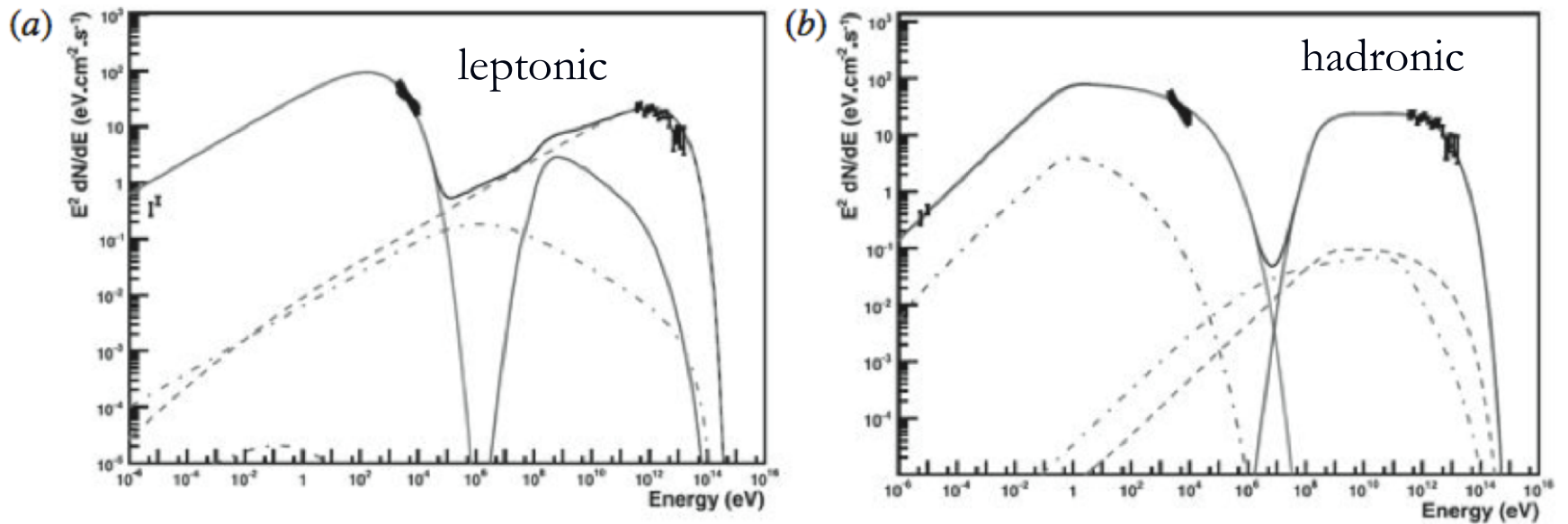


FIG. 4.5: Photon spectrum observed in radio, X-rays and γ -ray (HESS) from the RX J0852.0-4622 (Vela-Jr) SNR. Data points are compared with predictions assuming a leptonic (left) and a hadronic (right) origin of the γ -ray emission (see text).

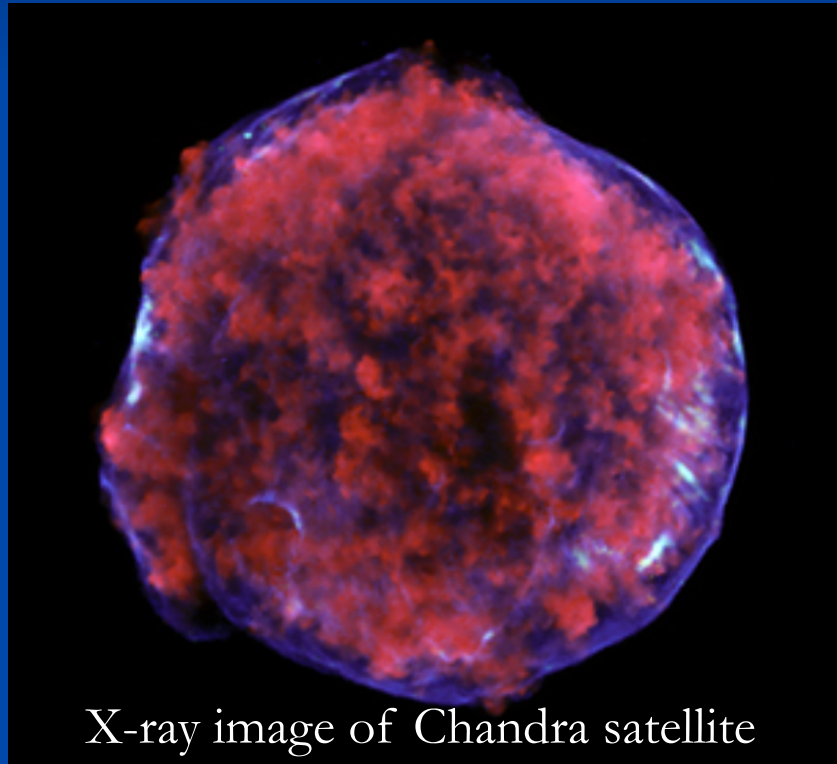
Leptonic/hadronic γ emission: RX J0852.0-4622 (Vela-Jr) SNR

The paucity of the informations on the SNR environment (as in 2007) as well as the very partial measurements of the multiwavelength photon spectrum makes the origin of the γ -ray signal difficult to determine with certainty. Let us note that, even assuming a hadronic origin of the γ -ray photons the fact that no photons were detected above ~ 20 TeV ($2 \cdot 10^{13}$ eV) implies that there is in any case no signature of the acceleration of cosmic-rays above a few 10^{14} eV, which represents an energy scale \sim an order of magnitude below the knee energy.

We started our brief tour of SNR observations by a relatively ambiguous case. For some SNRs the distinction between the leptonic or hadronic origin of the high energy photon signal can however be much clearer.

The Tycho SNR

The Tycho SNR is very well known, it corresponds to the remnant of the Tycho supernova which could be observed with the naked eyes in the years 1572.



X-ray image of Chandra satellite

The Tycho SNR

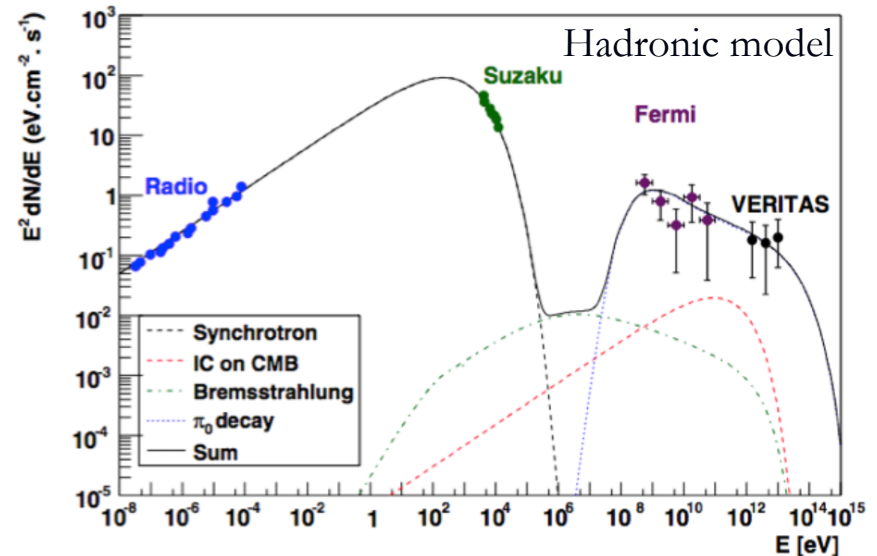
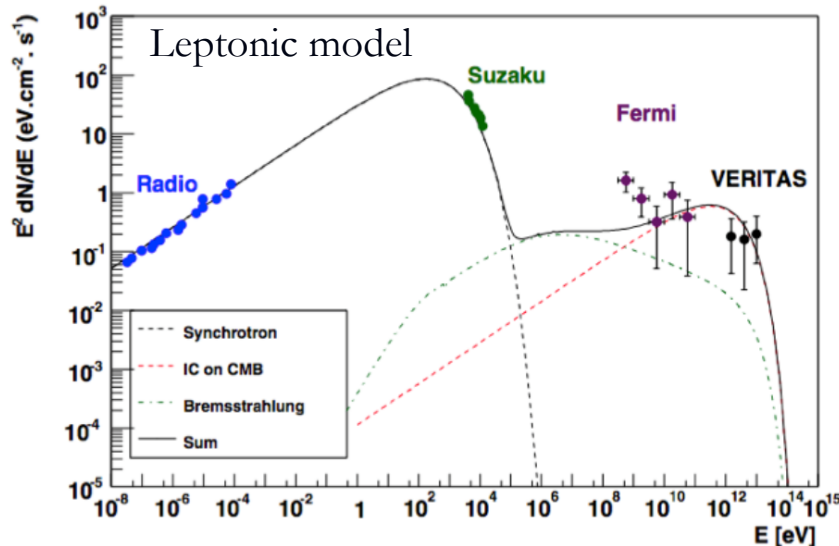
The emission spectrum is

now well measured in radio and X-rays (these emissions are interpreted as the synchrotron emission of accelerated electrons) allowing to constrain the value of the ambient magnetic which is found to be of the order of $B \sim 215 \mu\text{G}$ (which correspond to a strong amplification with respect to the ISM magnetic field). With such an important constraint, the determination of the origin of the γ -ray signal measured by both Fermi (below 100 GeV) and VERITAS (above 100 GeV) is easier although the distance of the remnant is not precisely known. As shown in Fig. 4.6, the best fit of

The Tycho SNR

The best fit of the multiwavelength data are obtained with models assuming a dominant contribution of hadronic processes. the spectral index found for the accelerated protons is $p \sim 2.3$ which is, as it should be (at least assuming acceleration by DSA), the same as the one of the electrons constrained by radio and X-ray data.

Leptonic models on the other hand give a much worse agreement with the data even though the model displayed allowed for a significant decrease of the assumed magnetic field (with respect to the favored value of $B \leftarrow 215 \mu\text{G}$)



Tycho SNR thus represent a case where we have very strong evidence of the acceleration of cosmic-rays in a SNR. Let us note however that no photon signal is observed above a few 10 TeV which means again that there is no signature of the acceleration of cosmic-rays above a few 10^{14} eV in this SNR

The RX J1713.7-3946 SNR

In the case of the SNR RX J1713.7-3946, a different conclusion is reached. This well known SNR is older than Tycho's SNR (~ 1700 years old) which means that this SNR is well within its Sedov phase (unlike Tycho's SNR which has entered the Sedov-Taylor phase). For RX J1713.7-3946, X-ray measurement point to a magnetic field of the order of $10 \mu\text{G}$ only slightly large than in the ISM. The γ -ray spectrum has been measured between $\sim 1 \text{ GeV}$ and 100 TeV by Fermi and HESS.

In this case, as can be seen in Fig. 4.7, it seems that leptonic models for which the γ -ray emission is dominated by the ICS emission of the accelerated electrons give a much better fit of the data. With such a low value of the magnetic field, it is indeed easier for the ICS emission to overwhelm the contribution from π^0 . The dominant contribution of the leptonic signal of course does not mean that cosmic-ray nuclei are not accelerated in this SNR, but there is no course no clear signature of this acceleration in the observed photon spectrum.

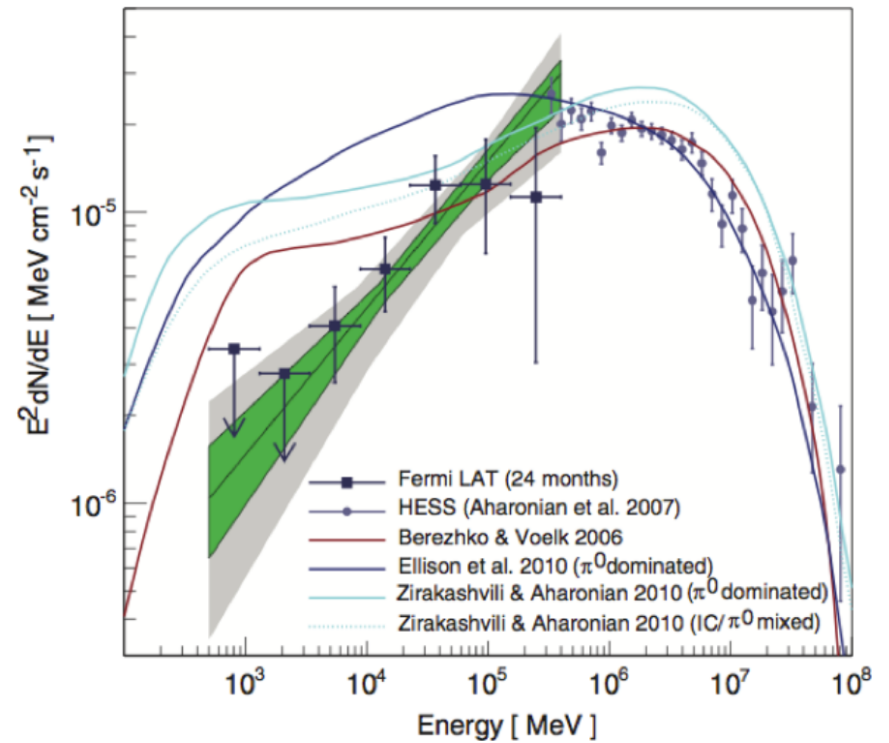
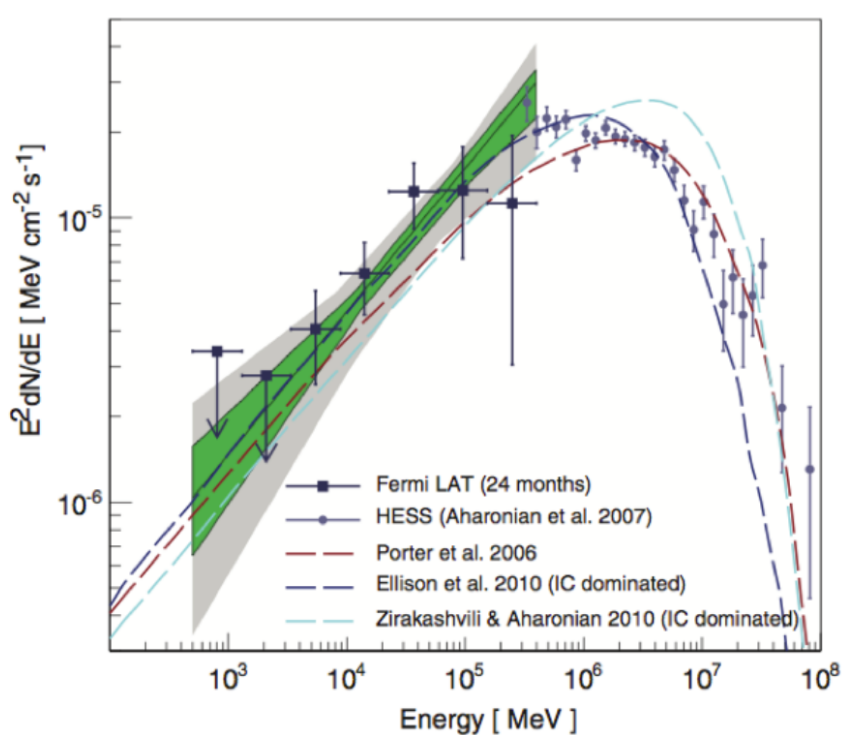
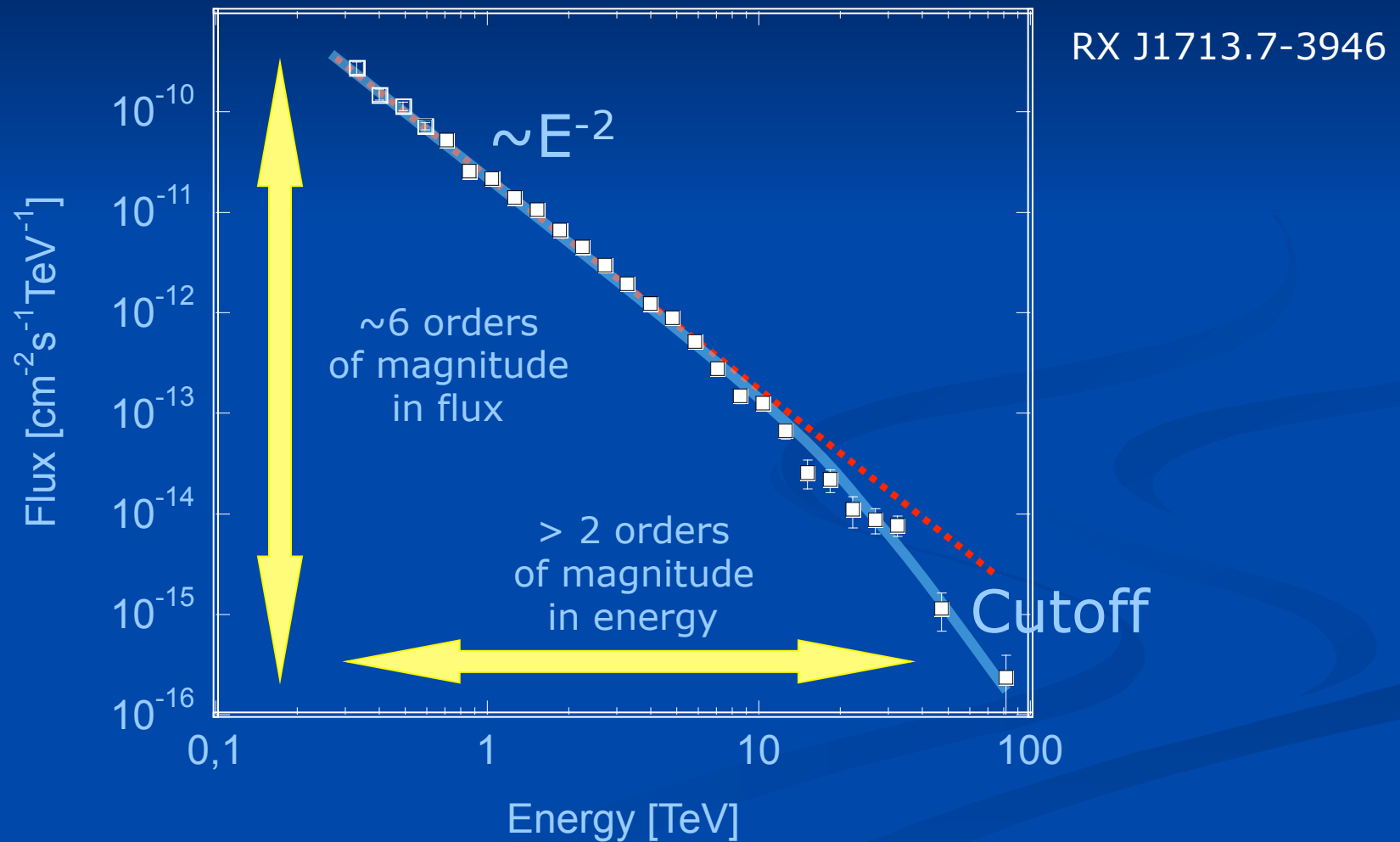


FIG. 4.7: Photon spectrum observed in γ -rays (Fermi and HESS) from the RX J1713.7-3946 SNR. Data points are compared with predictions assuming a leptonic (left) and a hadronic (right) origin of the γ -ray emission (see text).

Spettro energetico RX J1713.7-3946



SNRs and galactic cosmic rays

During the last few years and the emergence of high aperture and high resolution γ -ray observatories, the number of SNRs observed in γ -rays as well as the quality of the observations, increased significantly. A few tens of SNRs have now a well measured γ -ray photon spectrum. Among them some favour a leptonic origin of the signal while other favour a hadronic origin.

Although it is now clear that SNRs do accelerate some cosmic-rays ¹⁴, in the current situation it is extremely difficult to conclude on whether or not SNRs are the main sources of Galactic cosmic-rays. In particular, with current observations there is no photon signature of the fact that SNR are able to accelerate cosmic-rays beyond a few 10^{14} eV. Furthermore, the maximum energies of some SNRs (like Tycho and CasA) at the transition between the free expansion and the Sedov-Taylor phase as constrained by their X-ray rims seem indeed to be significantly lower than the knee energy. As we will see in the next few paragraphs this is in principle a problem since a good candidate for the title of "main source of the Galactic cosmic-rays" should be able to accelerate cosmic-rays at least up to the knee energy.

SNRs and galactic cosmic rays

Now one must be extremely careful in interpreting the γ -ray spectra, we just discussed since in principle they are representative of the accelerated particles population at a given time of the SNR evolution. These spectra are just telling us that at the (retarded) time of the observations, there is no sign of protons being accelerated above a few 10^{14} eV. It is not telling us anything about the population of cosmic-rays which are escaping to the ISM (since those that emit γ -ray are still inside the SNR), nor is it telling us anything about what the accelerated cosmic-ray population was at earlier times of the SNR evolution.

Taking at face value the toy model of a SNR evolution we discussed in the previous paragraphs, Tycho SNR or other well known and well observed SNRs like CasA, which are both more or less at the transition between the free expansion and the Sedov-Taylor, should be at the stage of their evolution at which the maximum energy of the accelerated cosmic-rays reaches its highest value. In the framework of this particular model of the SNR evolution the non observation of photon signature of the acceleration of cosmic-rays above 10^{14} eV would indeed indicate that they should never be able to reach much higher energies during their whole evolution.

SNRs and galactic cosmic rays

It is important to note that very different models for the evolution of the SNR, especially with respect to the maximum energy reachable by cosmic-rays have emerged in the past few years. Some of these models in particular predict that the production of very high energy cosmic-rays (well above 10^{15} eV) is possible during the very early times of the shock propagation (the very first few years or even on shorter time scales). These models invoke initially extremely strong magnetic fields (a few tens of Gauss !) decaying like t^{-1} (for which there exist some observational evidences in some rare type, exceptionally bright extragalactic supernovae). For this class of models it is normal not to observe any signature of cosmic-ray acceleration above 10^{15} eV since these signatures could only be found during a short period of time after the supernova event. The Galactic SNRs we observe in γ -rays all being much too old to present these signatures. Observation of larger samples of SNRs (especially younger SNRs) by the next generation of γ -ray observatory will certainly be required to further test the relevance of these more recent models. Molecular clouds we will discuss in the next paragraph also represent potentially powerful probes of both the cosmic-ray escape and the maximum acceleration energy.

SNRs and galactic cosmic rays

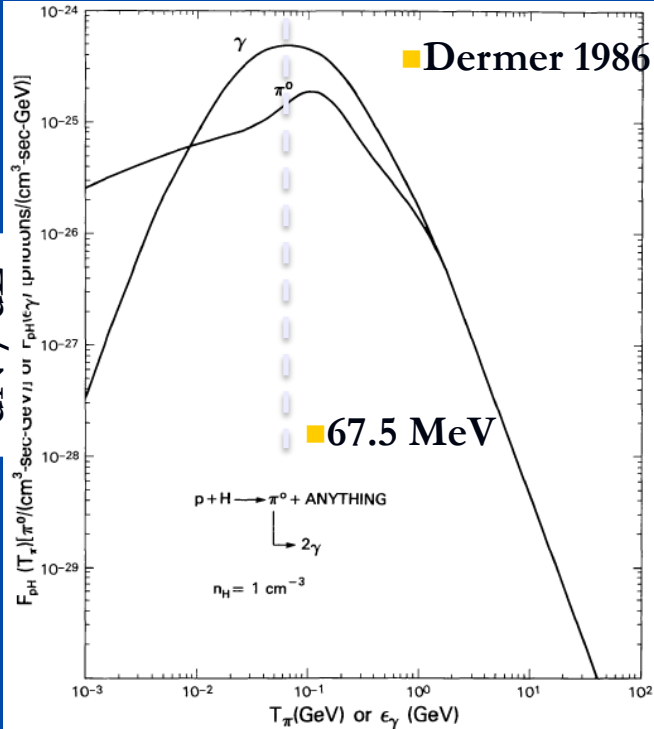
We must conclude that the nature of the main source of Galactic cosmic-rays is currently unclear. Although SNR still remain the most popular candidate, some authors have argued that scenarios involving super bubbles could solve most of the caveats encountered with the SNR scenario 15 but observational signatures are still needed to lend further weight to this possibility.

Molecular clouds as diagnostic tool for the spectrum of escaping CR

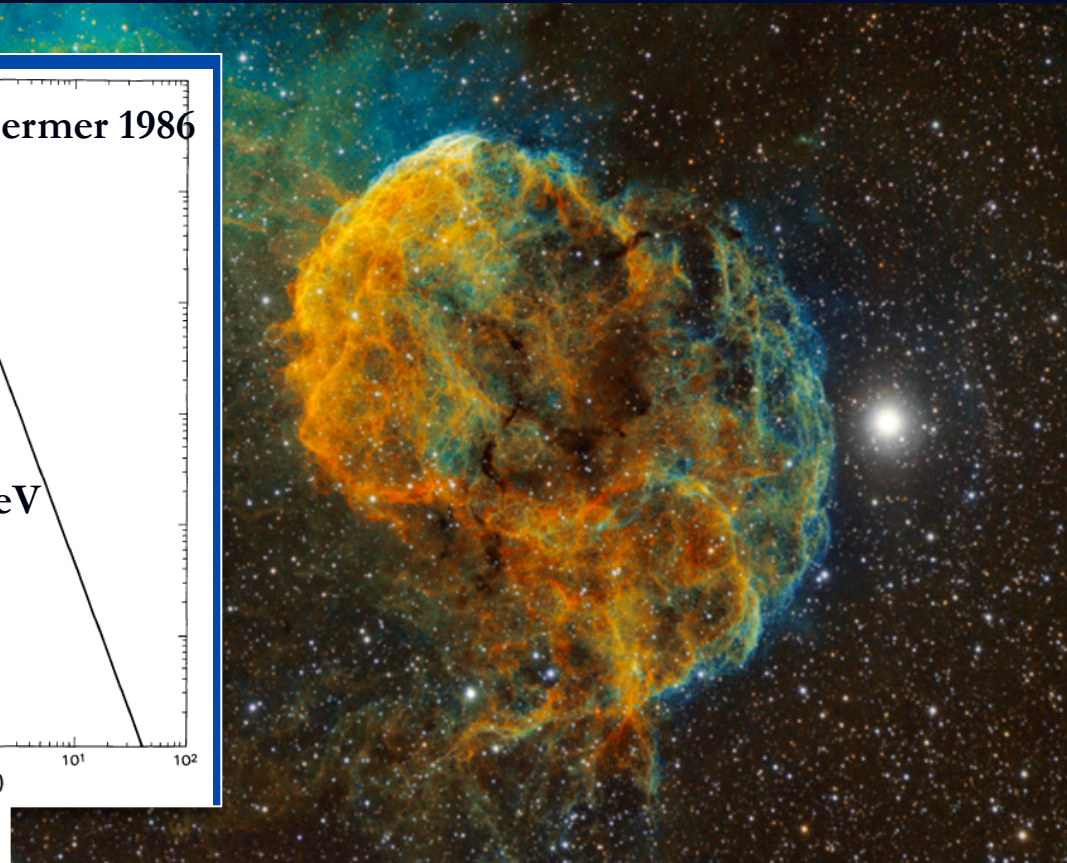
As discussed above multi-wavelength spectra give precious informations on the population of accelerated particles present in a SNR at a given time. Moreover, the observation of SNR of different ages gives us some hint of how these populations are evolving with time. However, these observations do not give any direct indication of the spectrum of cosmic-rays which are escaping from the SNR environment. This fact is of course problematic since these escaping cosmic-rays are precisely those which might eventually arrive on Earth after propagation in the ISM. As seen in Chapt. 1, the diffuse γ -ray emission associated with the Galactic plane is due to hadronic interactions of cosmic-rays with the ISM. Although this emission brings us informations on the propagation of these cosmic-rays in the Galaxy, this diffuse emission does not allow to put strong constraints on cosmic-ray origin.

Of course stronger γ -ray emission is expected denser regions of the ISM like molecular clouds (see Chapt. 1) which can locally reach densities of the order of 10^6 cm^{-3} . It is interesting to note that molecular cloud are often located in (or in the vicinity of) star forming regions meaning that there is a non negligible probability for molecular clouds to be found in the vicinity of SNRs. In this case, the flux of cosmic-rays entering the molecular cloud would be dominated by the contribution of the nearby SNR. The pp interactions in the molecular cloud and the consecutive γ -ray emission could be interpreted as the signature of escaping cosmic-rays from the nearby SNR environment and give precious informations about their energy.

dN / dE



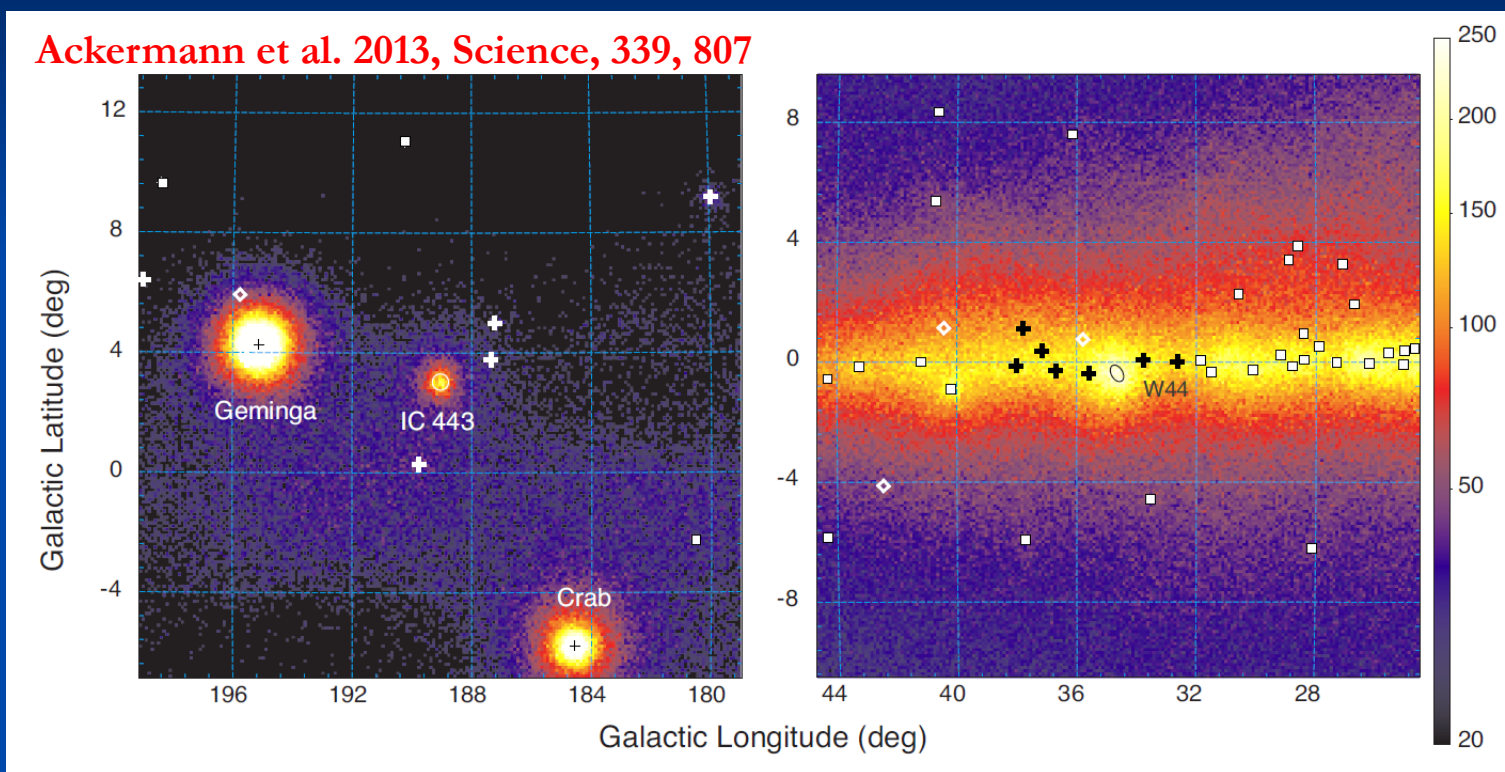
E_{gamma}



DETECTION OF THE PION- DECAY CUTOFF IN SUPERNOVA REMNANTS

Top SNR Candidates: IC 443 & W44

Both SNRs interacting with clouds, ages of $\sim 10^4$ years,

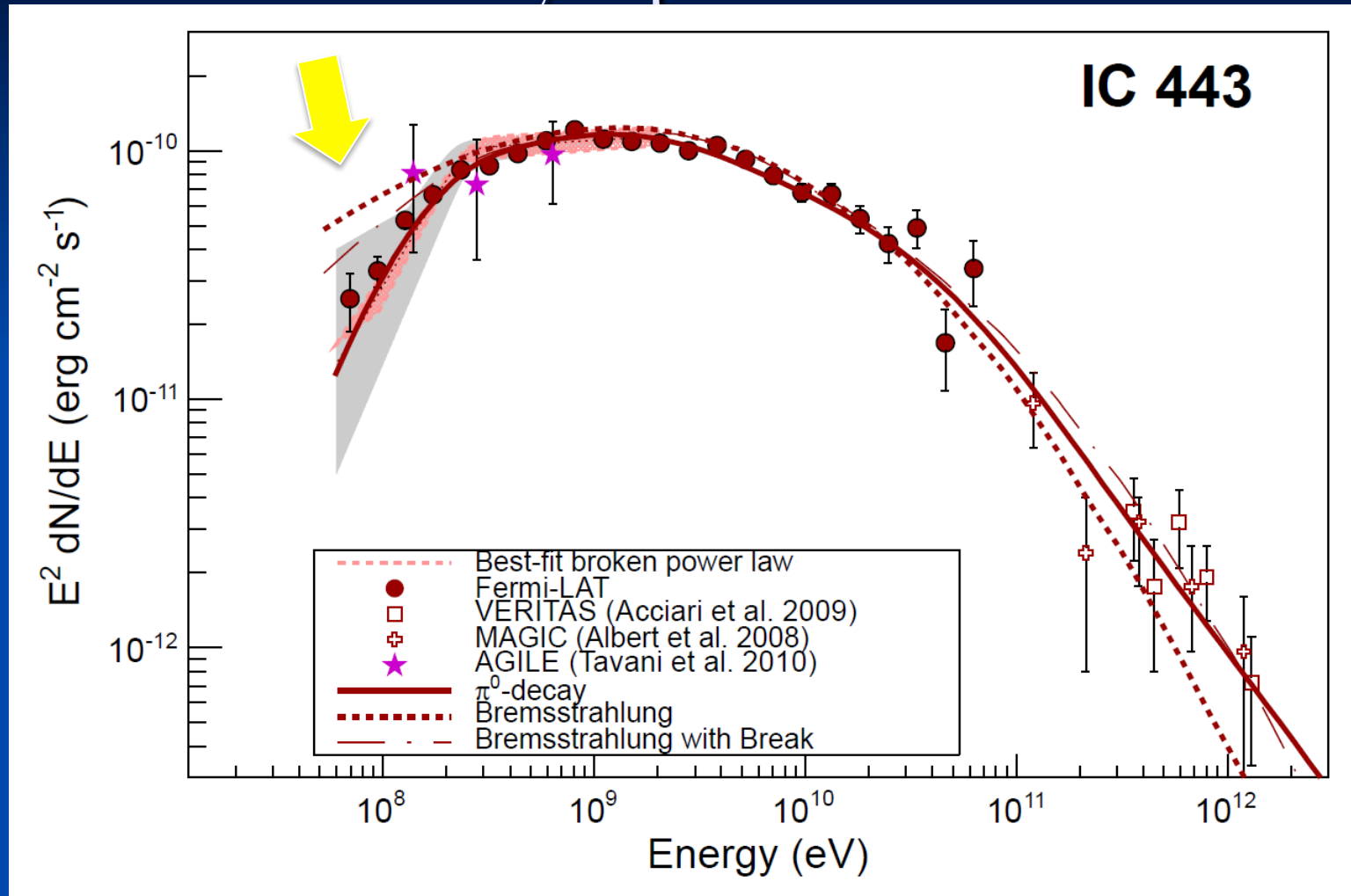


■ Counts map in 0.1 deg x 0.1 deg pixels, 60 MeV – 2 GeV

■ Diamonds indicate previously undetected sources

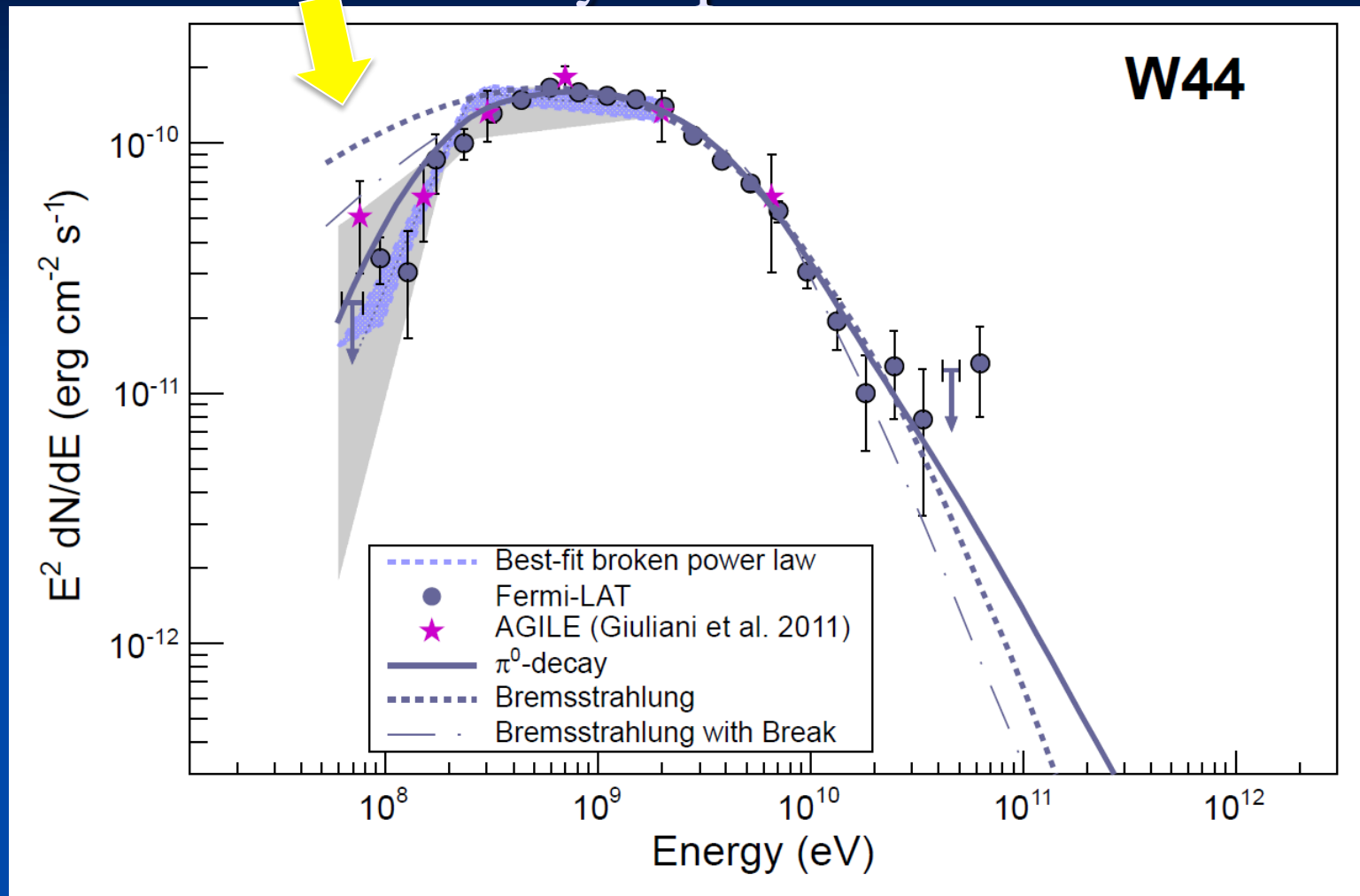
■ Crosses and diamonds indicate sources with normalization free in the fit

Gamma-ray Spectrum IC 443



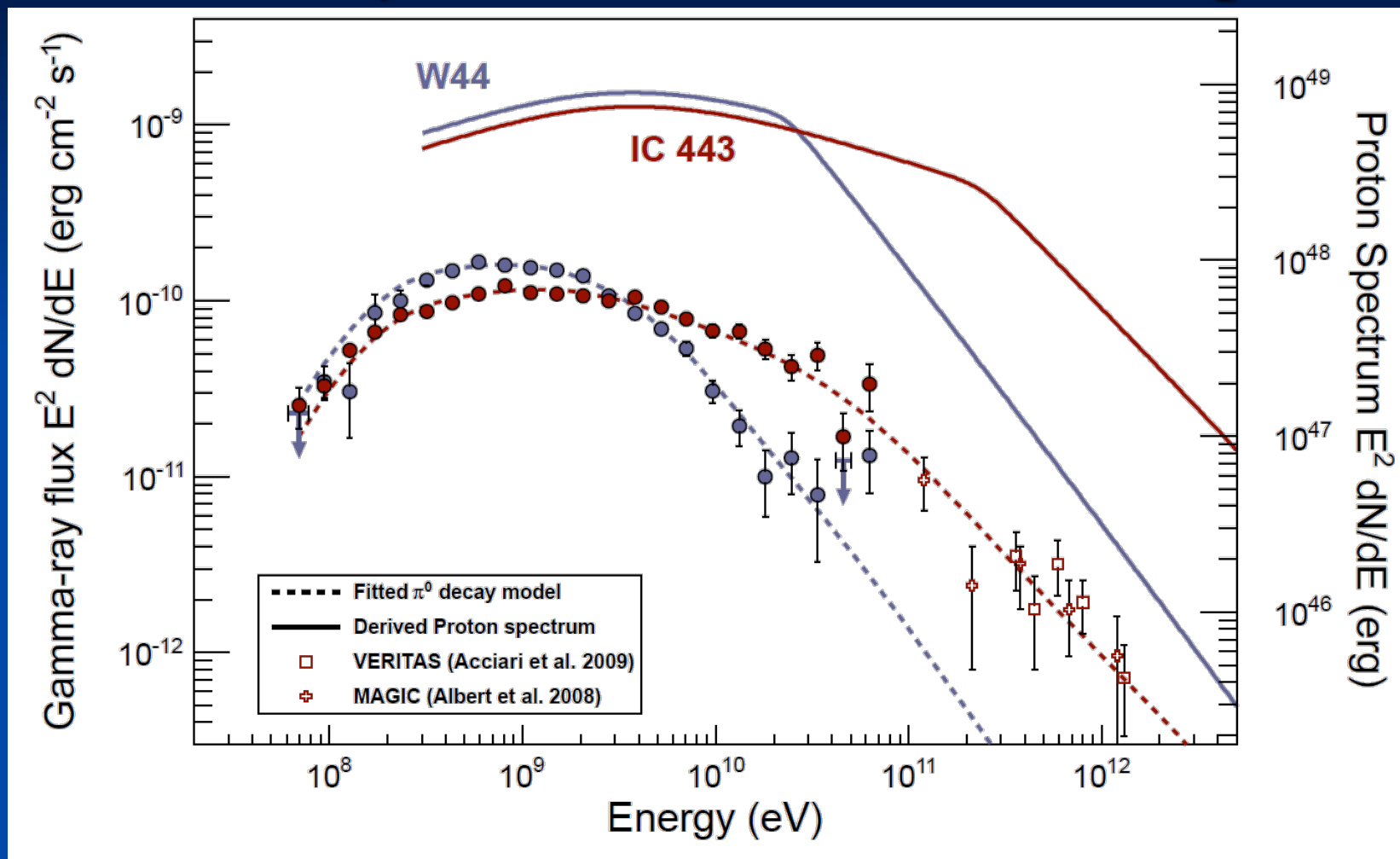
- Color (Gray) shaded region indicates statistical (systematic) uncertainty $< 2 \text{ GeV}$.
- Systematic uncertainty associated with Galactic diffuse modeling was estimated by using several alternative diffuse models based on GALPROP.
- Ackermann et al. 2013, Science, 339, 807

Gamma-ray Spectrum W44



- Color (Gray) shaded region indicates statistical (systematic) uncertainty < 2 GeV.
- Systematic uncertainty associated with Galactic diffuse modeling was estimated by using several alternative diffuse models based on GALPROP.
- Ackermann et al. 2013, Science, 339, 807

Gamma-ray and Inferred Proton Spectra



Assume average gas densities of 20 cm^{-3} (IC 443) and $n = 100 \text{ cm}^{-3}$ (W44) and distances of 1.5 kpc (IC 443) and 2.9 kpc (W44), factor 1.85 enhancement from heavier nuclei. Inferred CR acceleration efficiencies of 1-10% (protons with $p > 0.8 \text{ GeV c}^{-1}$).

The knee of the CR spectrum

Before closing our discussion of SNRs, it is useful to discuss the origin of the knee of the cosmic-ray spectrum to better understand some aspects we discussed in the previous paragraphs. We first remind that in the context of the leaky box model assuming a steady state we obtained in Chapt. 2, for a given nuclear species i :

$$0 = q_i(R) - \frac{N_i(R)}{\tau_{esc}(R)} \Leftrightarrow N_i(R) = q_i(R)\tau_{esc}(R) \quad (4.26)$$

The knee is a feature of the cosmic-ray spectrum (a steepening) observed on earth (see Fig. 4.13), one sees in Eq. 4.26 that this feature can come either from a change in the source term or in the escape term.

The knee of the CR spectrum

(i) In the case, the source term is involved, one could guess that the main sources of Galactic cosmic-rays are reaching their maximum energy at the knee, causing a feature in the spectrum. In this case, since the different species are expected to be accelerated to the same maximum rigidity (since we showed that energy losses were likely not to be a limiting factor for Galactic cosmic-ray acceleration), then the knee would more precisely mark the maximum energy of the proton component (which is the most abundant species), followed by the other species at energies $E_{max}(Z) = Z \times E_{max}(proton) = Z \times E_{knee}$. This behaviour is schematized in Fig. 4.13, where fictitious spectra of the most abundant species are depicted for illustrative purpose. Let us note that in this case, even if the proton component has a sharp cut-off above its maximum energy, the total spectrum will remain relatively smooth since the different species will experience their own knee at energies which are proportional to their charge.

Now of course, for this scenario to hold one needs the main sources of Galactic cosmic-rays to be able to accelerate protons at least up to the knee energy, which seems to be a bit challenging for SNR at least for models predicting that the highest value of the maximum energy is reached at the transition between the free expansion and the Sedov-Taylor phases.

(ii) On the other hand, it is also possible that the knee could be due to a change in the energy evolution of the escape term. In Chapt. 2, we saw that $\tau_{esc}(R) \propto D(R)^{-1}$ where D is the diffusion coefficient. We also saw that the rigidity evolution of the diffusion coefficient was expected to show an inflexion^{*} around the rigidity at which $r_L(R) \simeq \lambda_c$ (λ_c , being the coherence length of the field) as can be seen in Fig. 2.9. In the Galaxy we have roughly $B \simeq 3 - 10 \mu\text{G}$ and $\lambda_c \simeq 1 - 10\text{pc}$. Taking the values $3 \mu\text{G}$ and $\lambda_c = 1 \text{ pc}$ we see that the rigidity for which $r_L(R) \simeq \lambda_c$ is $\sim 3 \cdot 10^{15} \text{ V}$ which is close to the knee energy (for protons). Assuming the knee is indeed due a change in the rigidity evolution of the diffusion coefficient, since the rigidity is the relevant parameter, we would also expect first a change in the proton component and then changes in the behaviour of the other species at energies proportional to their charge (the schematic view in Fig. 4.13 would still hold qualitatively¹⁶).

Assuming the knee is purely due to the evolution of $\tau_{esc}(R)$ (and then of $D(R)$) then the source term would have to remain unchanged at the knee meaning that in this case the maximum energy of the main sources of Galactic cosmic-rays would have to be higher than the knee and probably even significantly higher. This eventuality is of course even more problematic for SNRs.

^{*}The diffusion coeff may vary if the magnetic field power spectrum changes

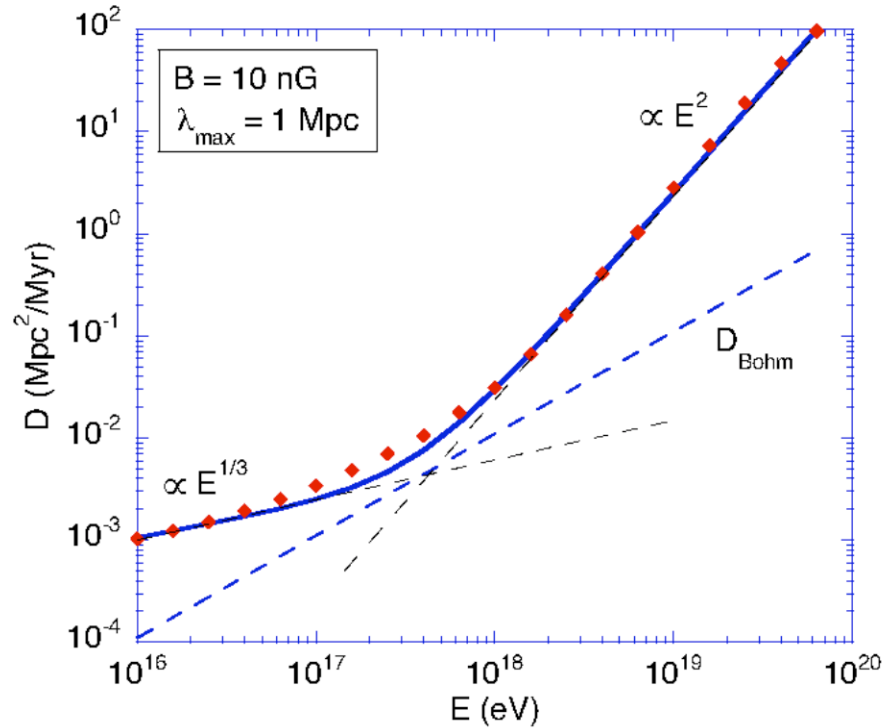


FIG. 2.9: Diffusion coefficient of protons as a function of energy, for a turbulent magnetic field $B = 10 \text{ nG}$ and $\lambda_{\text{max}} = 1 \text{ Mpc}$. The red dots are the computation results, with asymptotic behaviors indicated by the thin dashed lines. The Bohm diffusion coefficient is also shown for comparison (dashed line), the latter can be disregarded until we come to Chapter 3.

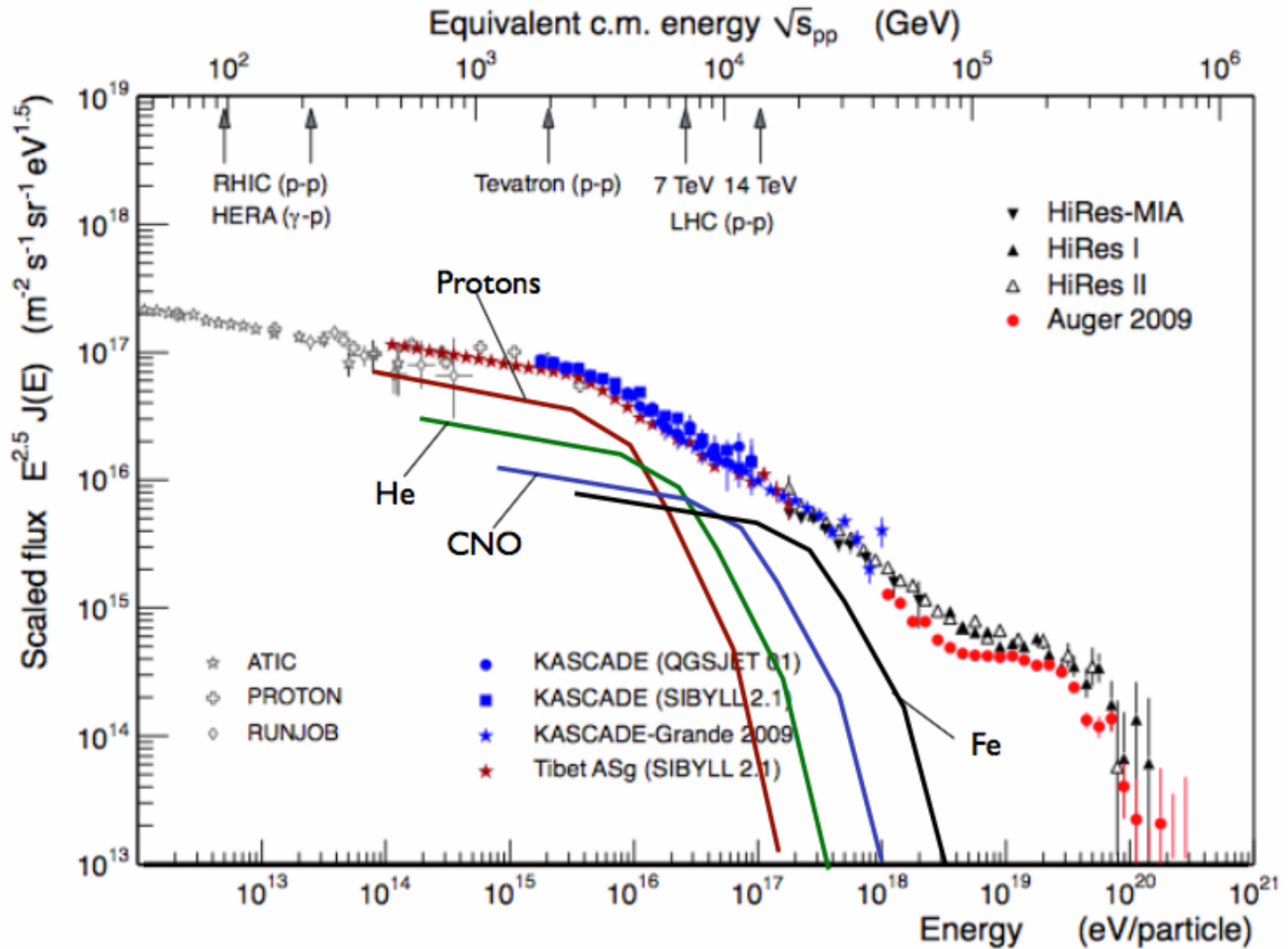


FIG. 4.13: Same as Fig. 2.2. In addition fictitious spectra of the most abundant species have been added to illustrate the idea of the successive knees of the different species at energies $E_{knee}(Z) = Z \times E_{knee}(\text{proton}) = Z \times E_{knee}$.